

## MASSIVE PERTURBER-DRIVEN INTERACTIONS OF STARS WITH A MASSIVE BLACK HOLE

HAGAI B. PERETS, CLOVIS HOPMAN<sup>1</sup> AND TAL ALEXANDER<sup>2</sup>  
Faculty of Physics, Weizmann Institute of Science, POB 26, Rehovot 76100, Israel  
*Draft version 5th July 2021*

### Abstract

We study the role of massive perturbers (MPs) in deflecting stars and binaries to almost radial (“loss-cone”) orbits, where they pass near the central massive black hole (MBH), interact with it at periaapse, and are ultimately destroyed. MPs dominate dynamical relaxation when the ratio of the 2nd moments of the MP and star mass distributions,  $\mu_2 \equiv N_p \langle M_p^2 \rangle / N_* \langle M_*^2 \rangle$ , satisfies  $\mu_2 \gg 1$ . We compile the MP mass function from published observations, and show that MPs in the nucleus of the Galaxy (mainly giant molecular clouds), and plausibly in late type galaxies generally, have  $10^2 \lesssim \mu_2 \lesssim 10^8$ . MPs thus shorten the relaxation timescale by  $10^{2-7}$  relative to 2-body relaxation by stars alone. We show this increases by  $10^{1-3}$  the rate of *large*-periaapse interactions with the MBH, where loss-cone refilling by stellar 2-body relaxation is inefficient. We extend the Fokker-Planck loss-cone formalism to approximately account for relaxation by rare encounters with MPs. We show that binary stars–MBH exchanges driven by MPs can explain the origin of the young main sequence B stars that are observed very near the Galactic MBH, and increase by orders of magnitude the ejection rate of hyper-velocity stars. In contrast, the rate of *small*-periaapse interactions of single stars with the MBH, such as tidal disruption, is only increased by a factor of a few. We suggest that MP-driven relaxation plays an important role in the 3-body exchange capture of single stars on very tight orbits around the MBH. These captured stars may later be disrupted by the MBH via tidal orbital decay or direct scattering into the loss cone; captured compact objects may inspiral into the MBH by the emission of gravitational waves from zero-eccentricity orbits.

*Subject headings:* black hole physics — clusters — galaxies: nuclei — stars: kinematics — giant molecular clouds

### 1. INTRODUCTION

There is compelling evidence that massive black holes (MBHs) lie in the centers of all galaxies (Ferrarese & Merritt 2000; Gebhardt et al. 2003; Shields et al. 2003), including in the center of our Galaxy (Eisenhauer et al. 2005; Ghez et al. 2005). The MBH affects the dynamics and evolution of the galaxy’s center as a whole (e.g. Bahcall & Wolf 1976) and it also strongly affects individual stars or binaries that approach it. Such close encounters, which may be extremely energetic, or involve non-gravitational interactions, or post-Newtonian effects, have been the focus of many studies (see review by Alexander 2005). These processes include the destruction of stars by the MBH, either by falling whole through the event horizon, or by being first tidally disrupted and then accreted (e.g. Rees 1988); tidal scattering of stars on the MBH (Alexander & Livio 2001); the capture and gradual inspiral of stars into the MBH, accompanied by the emission of gravitational waves or by tidal heating (e.g. Alexander & Hopman 2003; Alexander & Morris 2003); or dynamical exchange interactions in which incoming stars or binaries energetically eject a star tightly bound to the MBH and are captured in its place very near the MBH (e.g. Alexander & Livio 2004; Gould & Quillen 2003).

The interest in such processes is driven by their possible implications for the growth of MBHs, for the orbital decay of a MBH binary, for the detection of MBHs, for gravitational wave (GW) astronomy, as well as by observations of unusual stellar phenomena in our Galaxy, e.g. the puzzling young population of B-star very near the Galactic MBH (Eisenhauer et al. 2005), or the hyper-velocity B stars at the

edge of the Galaxy (Brown et al. 2005; Fuentes et al. 2006; Brown et al. 2006a), possibly ejected by 3-body interactions of a binaries with the MBH (Hills 1991).

Here we focus on close encounters with the MBH whose ultimate outcome (“event”) is the elimination of the incoming object from the system, whether on the short infall (dynamical) time, if the event is prompt (e.g. tidal disruption or 3-body exchange between a binary and the MBH), or on the longer inspiral time, if the event progresses via orbital decay (e.g. GW emission or tidal capture and heating). Such processes are effective only when the incoming object follows an almost zero angular momentum (“loss-cone”) orbit with periaapse closer to the MBH than some small distance  $q$ . To reach the MBH, or to decay to a short period orbit, both the infall and inspiral times must be much shorter than the system’s relaxation time  $t_r$  (Alexander & Hopman 2003). The fraction of stars initially on loss-cone orbits is very small and they are rapidly eliminated. Subsequently, the close encounter event rate is set by the dynamical processes that refill the loss-cone.

The loss-cone formalism used for estimating the event rate (Frank & Rees 1976; Lightman & Shapiro 1977; Cohn & Kulsrud 1978) usually assumes that the system is isolated and that the refilling process is 2-body relaxation. This typically leads to a low event rate, set by the long 2-body relaxation time.

Two-body relaxation, which is inherent to stellar systems, ensures a minimal loss-cone refilling rate. Other, more efficient but less general refilling mechanisms were also studied with the aim of explaining various open questions (e.g. the stalling problem of MBH binary coalescence, Berczik et al. (2005); Merritt & Wang (2005); Berczik et al. (2006), or MBH feeding, Zhao et al. 2002; Miralda-Escudé & Kollmeier 2005) or in the hope that they may lead to significantly higher event rates for close encounter processes. These mechanisms

Electronic address: hagai.perets, clovis.hopman, tal.alexander@weizmann.ac.il

<sup>1</sup> also Leiden Observatory, P.O. box 9513, NL-2300 RA Leiden

<sup>2</sup> The William Z. & Eda Bess Novick career development chair

include chaotic orbits in triaxial potentials (Norman & Silk 1983; Gerhard & Binney 1985; Merritt & Poon 2004; Holley-Bockelmann & Sigurdsson 2006) (the presence of a MBH may however destroy the triaxiality near the center; Merritt & Quinlan 1998; Holley-Bockelmann et al. 2002; Sellwood 2002); increased fraction of low angular momentum orbits in non-spherical potentials (Magorrian & Tremaine 1999; Berczik et al. 2006); accelerated resonant relaxation of angular momentum near the MBH where the orbits are Keplerian (Rauch & Tremaine 1996; Rauch & Ingalls 1998; Hopman & Alexander 2006a; Levin 2006); perturbations by a massive accretion disk or an intermediate mass black hole (IMBH) companion (Polnarev & Rees 1994; Zhao et al. 2002; Levin et al. 2005). Most of these mechanisms require special circumstances to work (e.g. specific asymmetries in the potential), or are short-lived (e.g. the IMBH will eventually coalesce with the MBH).

Here we explore another possibility, which is more likely to apply generally: accelerated relaxation and enhanced rates of close encounters driven by massive perturbers (MPs). Efficient relaxation by MPs was first suggested by Spitzer & Schwarzschild (1951, 1953) to explain stellar velocities in the galactic disk. MPs remain an important component in modern models of galactic disk heating (see e.g. Villumsen 1983, 1985; Lacey 1984; Jenkins & Binney 1990; Hänninen & Flynn 2002 and references therein). A similar mechanism was suggested to explain the spatial diffusion of stars in the inner Galactic bulge (Kim & Morris 2001). In addition to dynamical heating, efficient relaxation by MPs was suggested as a mechanism for loss cone replenishment and relaxation, both in the context of scattering of Oort cloud comets to the Sun (Hills 1981; Bailey 1983) and the scattering of stars to a MBH in a galactic nucleus (Zhao et al. 2002). Zhao et al. (2002) suggested MPs as a mechanism for establishing the  $M_\bullet/\sigma$  relation (Ferrarese & Merritt 2000; Gebhardt et al. 2000) by fast accretion of stars and dark matter. They also noted the possibility of increased tidal disruption flares and accelerated MBH binary coalescence due to MPs. In this study we investigate in detail the dynamical implications of loss-cone refilling by MPs. We evaluate its effects on the different modes of close interactions with the MBH, in particular 3-body exchanges, which were not considered by Zhao et al. (2002), and apply our results to the Galactic Center (GC), where observations indicate that dynamical relaxation is very likely dominated by MPs.

This paper is organized as follows. In §2 we present the main concepts and procedures of our calculations. The observational data and theoretical predictions about MPs in the inner  $\sim 100$  pc of the GC are reviewed in §3. In section §4 we explore the implications of relaxation by MPs for various types of interactions with the MBH. We summarize our results in §5.

## 2. LOSS-CONE REFILLING

In addition to stars, galaxies contain persistent dense structures<sup>3</sup> such as molecular clouds, open clusters and globular clusters with masses up to  $10^4\text{--}10^7 M_\odot$ . Such structures can perturb stellar orbits around the MBH much faster than 2-body stellar relaxation (hereafter “stellar relaxation”), provided they are numerous enough. This condition can be quantified by considering a test star randomly scattered by

perturbers with masses in the interval  $(M_p, M_p + dM_p)$  and number density  $(dN_p/dM_p)dM_p$ , approaching it with relative velocity  $v$  on orbits with impact parameters in the interval  $(b, b + db)$ . The minimal impact parameter still consistent with a small angle deflection is  $b_{\min} = GM_p/v^2$  (the capture radius), where  $v$  is of the order of the local velocity dispersion  $\sigma$ . Defining  $B \equiv b/b_{\min} \geq 1$ , the encounter rate is then

$$\begin{aligned} \left(\frac{d^2\Gamma}{dM_p db}\right) dM_p db &\sim \left(\frac{dN_p}{dM_p}\right) dM_p v b_{\min}^2 2\pi B dB \\ &= \frac{G^2}{v^3} \left[\left(\frac{dN_p}{dM_p}\right) M_p^2\right] dM_p 2\pi B dB. \end{aligned} \quad (1)$$

The total rate is obtained by integrating over all MP masses and over all impact parameters between  $b_{\min}$  and  $b_{\max}$ . Here we are interested in perturbations in the specific angular momentum  $J$  of a star relative to the central MBH, and so  $b_{\max} \sim r$ , the radial distance of the star from the center. MPs with substantially larger impact parameters are much less efficient because their effect on the MBH-star pair is tidal rather than direct.

The relaxation rate due to all MPs at all impact parameters is then

$$\begin{aligned} t_r^{-1} &= \int_{b_{\min}}^{b_{\max}} db \int dM_p \left(\frac{d^2\Gamma}{dM_p db}\right) \\ &\sim \log \Lambda \frac{G^2}{v^3} \int dM_p \left(\frac{dN_p}{dM_p}\right) M_p^2, \end{aligned} \quad (2)$$

where  $\log \Lambda = \log(b_{\max}/b_{\min})$  is the Coulomb logarithm (here the dependence of  $\log \Lambda$  and  $v$  on  $M_p$  is assumed to be negligible). For stars, typically  $\log \Lambda \gtrsim 10$ ; the omission of large angle scattering by encounters with  $b < b_{\min}$  is thus justified because it introduces only a relatively small logarithmic correction. This formulation of the relaxation time is equivalent to its conventional definition (Spitzer 1987) as the time for a change of order unity in  $v^2$  by diffusion in phase space due to scattering,  $t_r \sim v^2/D(v^2)$ , where  $D(v^2)$  is the diffusion coefficient.

If the stars and MPs have distinct mass scales with typical number densities  $N_\star$  and  $N_p$  and rms masses  $\langle M_\star^2 \rangle^{1/2}$  and  $\langle M_p^2 \rangle^{1/2}$  ( $\langle M^2 \rangle \equiv \int M^2 (dN/dM) dM/N$ ), then MPs dominate if the ratio of the 2nd moments of the MP and star mass distributions,  $\mu_2 \equiv N_p \langle M_p^2 \rangle / N_\star \langle M_\star^2 \rangle$ , satisfies  $\mu_2 \gg 1$  (note that for a continuous mass spectrum, this condition is equivalent to  $-\text{d} \log N / \text{d} \log M < 2$ ).

As discussed in detail in §3, the central  $\sim 100$  pc of the Galactic Center (GC) contain  $10^8 - 10^9$  solar masses in stars, and about  $10^6 - 10^8$  solar masses in MPs such as GMCs or open clusters of masses  $10^3 - 10^8 M_\odot$  (Oka et al. 2001; Figier et al. 2002, 2004; Vollmer et al. 2003; Güsten & Philipp 2004; Borissova et al. 2005). An order of magnitude estimate indicates that MPs in the GC can reduce the relaxation time by several orders of magnitude,

$$\begin{aligned} \frac{t_{r,\star}}{t_{r,\text{MP}}} &= \mu_2 \sim \frac{(N_p M_p) M_p}{(N_\star M_\star) M_\star} \\ &= 10^4 \left[ \frac{(N_\star M_\star / N_p M_p)}{10} \right]^{-1} \left[ \frac{(M_p / M_\star)}{10^5} \right]. \end{aligned} \quad (3)$$

Note that  $\mu_2$  does not include possible modifications in the value of  $\log \Lambda$  for MPs due to their much larger size, which may decrease this ratio by  $O(10)$ . This estimate is borne by more detailed calculations (Fig. 1 and table 2), using the formal definition  $t_r = v^2/D(v_\parallel^2)$  with  $M_\star \rho_\star \rightarrow$

<sup>3</sup> Structures that persist at least as long as the local galactic dynamical time and are substantially denser than the ambient stellar mass distribution.

$\int (dN_p/dM_p) M_p^2 dM_p$  (e.g. Binney & Tremaine 1987, Eqs. 8-69 to 8-70). A similar result is indicated by simulations of spatial diffusion of stars in the central 100 pc (Kim & Morris 2001).

### 2.1. Non-coherent loss-cone refilling

The Fokker-Planck approach to the loss-cone problem (e.g. Cohn & Kulsrud 1978) assumes that the effects of multiple small perturbations on the orbit of a test star dominate over the rarer strong close encounters ( $b_{\max}/b_{\min} \gg 1$ ), and that the cumulative effect can be described as diffusion in phase space. The change in the angular momentum of the test star then grows non-coherently,  $\Delta J \propto \sqrt{t}$ . The change over one orbital period  $P$  is  $J_D = J_c(E) \sqrt{P/t_r}$ , where  $J_c = \sqrt{2(\psi - E)}r$  is the maximal (circular) angular momentum for a stellar orbit of specific relative energy  $E = -v^2/2 + \psi(r)$ , and  $\psi \equiv -\phi$  is the negative of the gravitational potential, so that  $E > 0$  for bound orbits. The magnitude of  $J_D$  relative to the  $J$ -magnitude of the loss-cone,

$$J_{lc} \simeq \sqrt{2GM_\bullet q}, \quad (4)$$

determines the mode of loss-cone refilling. The relative volume of phase space occupied by the loss-cone,  $J_{lc}^2/J_c^2(E)$ , increases with  $E$  (decreases with  $r$ ) while  $P$  decreases. Near the MBH (high  $E$ )  $J_D \ll J_{lc}$ , stars diffuse slowly into the loss-cone, and are promptly destroyed over an orbital period, leaving the loss-cone always nearly empty. In this empty loss-cone regime, the loss-cone is relatively large, but the refilling rate is set by the long relaxation timescale (e.g. Lightman & Shapiro 1977),

$$\left(\frac{d\Gamma}{dE}\right)_{\text{empty}} \simeq \frac{N_\star(E)}{\log(J_c/J_{lc})t_r} = \frac{J_D^2(E)}{J_c^2(E)} \frac{1}{\log[J_c(E)/J_{lc}]} \frac{N_\star(E)}{P(E)}, \quad (5)$$

where  $N_\star(E)$  is the stellar number density per energy interval.

Far from the MBH (low  $E$ )  $J_D \gg J_{lc}$ , stars diffuse across the loss-cone many times over one orbit, and the loss cone is always nearly full. In this full loss-cone regime the refilling rate is set by the short orbital time, but the loss cone is relatively small,

$$\left(\frac{d\Gamma}{dE}\right)_{\text{full}} \simeq \frac{J_{lc}^2}{J_c^2(E)} \frac{N_\star(E)}{P(E)}. \quad (6)$$

Note that here and elsewhere we make the simplifying approximation that the period is a function of energy only, which is true only for motion in a Keplerian potential.

The total contribution to loss-cone refilling is dominated by stars with energies near the critical energy  $E_c$  (equivalently, critical typical radius  $r_c$ ) separating the two regimes (Lightman & Shapiro 1977; see §4). Within  $r_c$  ( $E > E_c$ ), an object, once deflected into the loss cone, can avoid being scattered out of it before reaching the MBH<sup>4</sup>. The empty and full loss-cone regimes of infall processes can be interpolated

<sup>4</sup> In the case of inspiral,  $E_c$  is determined by the condition  $J_D = J_{lc}$  over the inspiral time, rather than the much shorter orbital period, which results in a much smaller  $r_c$  than for direct infall. Inspiring stars with  $E > E_c$  can avoid being scattered directly into the MBH before completing the orbital decay. There is no contribution to inspiral events from regions outside  $r_c$  ( $E < E_c$ ), since the probability of an object to remain on its low- $J$  trajectory over the many orbital periods required to complete the inspiral, is vanishingly small.

to give a general approximate expression for the differential event rate for these non-coherent encounters (e.g. Young 1977),

$$\frac{d\Gamma}{dE} \simeq \frac{j^2(E)}{J_c^2(E)} \frac{N_\star(E)}{P(E)}, \quad (7)$$

with

$$j^2(E) \equiv \min \left[ \frac{J_D^2(E)}{\log(J_c(E)/J_{lc})}, J_{lc}^2 \right], \quad (8)$$

where  $j$  is the loss-cone limited angular momentum change per orbit, which expresses the fact that the loss-cone can at most be completely filled during one orbit.

### 2.2. Coherent loss-cone refilling

The loss-cone formalism can be generalized to deal with MPs in an approximate manner with only few modifications. The capture radius for MPs may be smaller than their size. Since the MP mass profile is centrally concentrated, we adopt the modified definition

$$b_{\min} = \min(0.1R_p, GM_p/v^2), \quad (9)$$

where  $v^2 = GM(< r)/r$ . This results in  $\log \Lambda \sim 6$  for MPs, less than the typical value for relaxation by stars. Nevertheless, the error introduced by neglecting encounters with  $b < b_{\min}$  is still not very large because penetrating encounters are much less efficient. However, the assumption of multiple non-coherent encounters with MPs over one orbital period is not necessarily justified because of their small number density.

To address this, we modify the treatment of the empty loss-cone regime (the contribution to the event rate from regions where the loss-cone is already filled by stellar relaxation can not be increased by MPs, see §4). We define rare encounters as those with impact parameters  $b \leq b_1$ , where  $b_1$  is defined by

$$P \int_{b_{\min}}^{b_1} db (d\Gamma/db) = 1. \quad (10)$$

The differential rate is estimated simply by  $(d\Gamma/db) = N_p v 2\pi b$ . When  $P \int_{b_1}^{b_{\max}} db (d\Gamma/db) > 1$ , with  $b_{\max} = r$ , all encounters with  $b > b_1$  are defined as frequent encounters that occur more than once per orbit, and add non-coherently<sup>5</sup>. Note that even when  $P \int_{b_1}^{b_{\max}} db (d\Gamma/db) > 1$  for all MPs, perturbations by rare, very massive MPs may still occur less than once per orbit. Our treatment is approximate. A complete statistical treatment of this situation lies beyond the scope of this study.

When the typical number of encounters per orbit is less than one, the fractional contributions from different individual encounters,  $\delta J$ , should be averaged coherently ( $\Delta J \propto t$ ), subject to the limit that each encounter can at most fill the loss-cone. The loss-cone limited change in angular momentum per orbit due to rare encounters is therefore

$$j_R^2(E) = \left[ P \int_{b_{\min}}^{b_1} db \frac{d\Gamma}{db} \min(\delta J, J_{lc}) \right]^2. \quad (11)$$

In contrast, frequent uncorrelated collisions add up non-coherently ( $\Delta J \propto \sqrt{t}$ ), and it is only their final value that

<sup>5</sup> In the marginal cases of  $P \int_{b_{\min}}^{b_{\max}} db (d\Gamma/db) < 1$  or  $P \int_{b_1}^{b_{\max}} db (d\Gamma/db) < 1$ , all encounters are considered rare.

is limited by the loss-cone (individual steps  $\delta J$  may exceed  $J_{lc}$ , but can then be partially cancelled by opposite steps during the same orbit). The loss-cone limited change in angular momentum per orbit due to frequent encounters is therefore

$$j_F^2(E) = \min \left[ \frac{1}{\log(J_c/J_{lc})} P \int_{b_1}^{b_{\max}} db \frac{d\Gamma}{db} \delta J^2, J_{lc}^2 \right]. \quad (12)$$

The total loss-cone limited angular momentum change per orbit is then approximated by

$$j^2 = \min (j_R^2 + j_F^2, J_{lc}^2), \quad (13)$$

and the differential event rate is calculated by Eq. (7),  $d\Gamma/dE = [j^2(E)/J_c^2(E)] N_*(E)/P(E)$ .

The contribution of rare encounters is evaluated in the impulse approximation by setting  $\delta J \sim GM_p r/bv$  in Eq. (11). We find that the this contribution by GC MPs (§3) is generally small. Frequent encounters are the regime usually assumed in the Fokker-Planck treatment of the loss-cone problem (e.g. Lightman & Shapiro 1977). To evaluate the contribution of frequent encounters, we do not calculate  $\delta J$  directly, but instead calculate the sub-expression  $I = P \int_{b_1}^{b_{\max}} db (d\Gamma/db) \delta J^2$  in Eq. (12) in terms of the  $b$ -averaged diffusion coefficient  $D(v_t^2)$ , after averaging over the orbit between the periape  $r_p$  and apoapse  $r_a$  and averaging over the perturber mass function (this is essentially equivalent to the definition of  $J_D$  in terms of  $t_r$ , §2.1),

$$\begin{aligned} I &= \int dM_p \left( 2 \int_{r_p}^{r_a} \frac{r^2 D(\Delta v_t^2)}{v_r} dr \right) \\ &\simeq \int dM_p \left( 2 \int_0^{2r} \frac{r^2 D(\Delta v_{\perp}^2)}{v} dr \right). \end{aligned} \quad (14)$$

The assumptions involved in the last approximate term (Magorrian & Tremaine 1999) are that the star is on a nearly radial orbit ( $v_r \rightarrow v$ ,  $r_p \rightarrow 0$ ,  $r_a \rightarrow 2r$ ) and that  $D(v_t^2)$  (the diffusion coefficient of the transverse velocity relative to the MBH) can be approximated by  $D(\Delta v_{\perp}^2)$  (the diffusion coefficient of the transverse velocity relative to the stellar velocity  $v$ ), given explicitly by (Binney & Tremaine (1987), Eq. 8-68)

$$D(\Delta v_{\perp}^2) = \frac{8\pi G^2 (dN_p/dM_p) M_p^2 \ln \Lambda}{v} K \left( \frac{v}{\sqrt{2}\sigma} \right), \quad (15)$$

where  $K(x) \equiv \text{erf}(x)(1 - 1/2x^2) + \exp(-x^2)/\sqrt{\pi}x$  and where a spatially homogeneous distribution of MPs with a Maxwellian velocity distribution of rms 1D velocity  $\sigma$  was assumed.

To summarize, the event rates are calculated as follows. For each perturber model (table 2), we integrate over the stellar distribution ( $N_* = 1.2 \times 10^6 (r/0.4 \text{ pc})^{-2}$ , for  $r > 0.4 \text{ pc}$  and  $M_* = 1 M_{\odot}$ ) in terms of  $r$ , using  $N_*$  to derive the appropriate density of perturbed objects (single stars §4.1 or binaries §4.2). At each  $r$  we calculate  $b_{\min}$  (Eq. 9),  $b_1$  (Eq. 10),  $j_R$  (Eq. 11) and  $j_F$  (Eq. 12). The integral  $I$  (Eq. 14) is evaluated by taking  $v^2 \rightarrow GM(<r)/r$  and correcting approximately for the difference relative to the exact calculation. We use  $j$  (Eq. 13) to calculate the differential event rate  $d\Gamma/dr$  (Eq. 7), with the *ansatz*  $E \rightarrow GM(<r)/2a$  where  $a \equiv (4/5)r$  is an effective semi-major axis, which is motivated by the fact that for a Keplerian isothermal eccentricity distribution,  $\langle r \rangle = a(1 + \langle e^2 \rangle/2) = (5/4)a$ . The total event rate is calculated by carrying the integration over  $r$  in the region where MPs exist, between  $r_{\text{MP}}$  and  $r_{\text{out}}$  (§3).

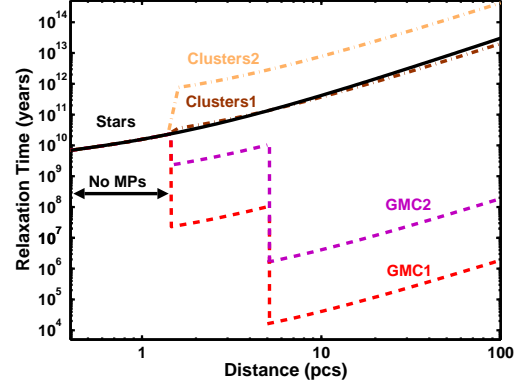


FIG. 1.— Relaxation time as function of distance from the MBH, for stars (solid line) and for each of the 4 MP models separately, as listed in table 2: clusters (dashed-dotted lines), GMCs (dashed lines). The discontinuities are artifacts of the assumed sharp spatial cutoffs on the MP distributions. 2-body stellar processes dominate close to the MBH, where no MPs are observed to exist. However, at larger distances massive clumps (at  $1.5 < r < 5 \text{ pc}$ ) and GMCs (at  $5 < r < 100$ ) are much more important.

### 3. MASSIVE PERTURBERS IN THE GALACTIC CENTER

MPs can dominate relaxation only when they are massive enough to compensate for their small space densities. Here we consider only MPs with masses  $M_p \geq 10^2 M_{\odot}$ . Such MPs could be molecular clouds of different masses, in particular giant molecular clouds (GMCs), open or globular stellar clusters, and perhaps also IMBHs. As discussed below, observations of the Galaxy reveal enough MPs to dominate relaxation in the central 100 pc. We adopt here a conservative approach, and include in our modeling only those MPs that are directly observed in the Galaxy, namely GMCs and young clusters. We discuss briefly theoretical predictions for two other classes of MPs: dynamically evolved “submerged” clusters and IMBHs, that could well be common in galactic centers and contribute to efficient relaxation.

The dynamically dominant MPs are GMCs. Emission line surveys of the central  $\sim 100 \text{ pc}$  reveal  $\sim 100$  GMCs with estimated masses in the range  $10^4 - 5 \times 10^7 M_{\odot}$  and sizes of  $R_p \sim \text{few pc}$  (Miyazaki & Tsuboi 2000; Oka et al. 2001; Güsten & Philipp 2004). We selected individual, reliably identified GMCs in the central  $0.7^\circ$  of the Galaxy ( $\sim 100 \text{ pc}$  of the GC), from the sample observed by Oka et al. (2001). Figure 2 shows the empirical GMC mass function using their virial mass estimates as an upper mass limit and adopting a lower limit 10 times smaller, following Miyazaki & Tsuboi (2000) who found that LTE mass estimates are typically an order of magnitude lower than the virial ones. Note that the more recent GMC CO1-0 molecular line observations by Oka et al. (2001), which we use here, indicate a more massive and flatter mass function than that derived for their earlier CS1-0 molecular line observations (Miyazaki & Tsuboi 2000). This is probably due to the higher sensitivity of the CO1-0 line to lower-density molecular gas (M. Tsuboi, priv. comm.).

Inside the inner 5 pc of the GC (a volume smaller or comparable to that of a GMC or a stellar cluster), the most massive local structures are the molecular gas clumps observed in the circumnuclear gaseous disk (CND) and its associated spiral-like structures (Genzel et al. 1985; Christopher et al. 2005). Their size are  $\sim 0.25 \text{ pc}$  and their masses are estimated to

be in the range  $10^3$ – $10^5 M_\odot$ , where the lower estimates are based on the assumption of optically thin HCN(1-0) line emission and the upper estimates are based on the optically thick assumption, which also coincides with the virial estimates.

It is possible to obtain a model-independent estimate of the effect of the *observed* MPs on the relaxation time by the directly derived value  $\mu_2^{\text{obs}} = \sum_i M_{p,i}^2 / N_* M_*^2$ , which is listed in table 2. The observed GMC masses show that  $\mu_2^{\text{obs}} \sim 2 \times 10^{6-8}$  on the 100 pc scale, and  $\mu_2^{\text{obs}} \sim 6 \times 10^{1-3}$  on the 5 pc scale, a clear indication that MPs dominate the relaxation on all relevant lengthscales, where MPs exist. For the purpose of our numeric calculations below, it is convenient to describe the differential mass function analytically. Here we adopt a power-law  $dN_p/dM_p \propto M_p^{-\beta}$  parameterization (or a lognormal probability distribution function (LNPDF) in the appropriate cases  $dN_p/dM_p \propto \text{LNPDF}(\mu, \sigma)$ , where  $\mu$  is the log mean and  $\sigma$  is the log standard deviation). Figure 2 shows that the power law distribution is a good fit for the GMCs mass function (Miyazaki & Tsuboi 2000), and for the lower estimates of the clusters and gas clumps. For the upper estimates of the clusters and the molecular gas clumps the MFs were found to be better fit by a lognormal distribution, which we used in these cases. It should be emphasized that our results and conclusions are determined primarily by the large values of  $\mu_2$ , and not by the detailed form of the mass function. We repeated our calculations with several alternative distributions and found qualitatively similar results. The assumed high mass cutoff of the MF is important, as it determines the magnitude of  $\mu_2$ . Figure 2 shows that our models do not extrapolate beyond the maximum observed MP masses (and even fall below them for GMCs).

We obtained best fit power indices  $\beta$  and LNPDF indices  $\mu$  and  $\sigma$  for the lower and upper estimates. The cumulative mass functions and best fits are shown in Fig. (2) and listed in table 1. We find  $\beta = 1.2$  for both the lower mass range ( $1.4 \times 10^4 \leq M_p \leq 5 \times 10^6 M_\odot$ ) and the upper GMC mass range ( $1.4 \times 10^5 \leq M_p \leq 5 \times 10^7 M_\odot$ ). The clump mass function has  $\beta \simeq 1.1$  for the lower mass range ( $2.4 \times 10^2 \leq M_p \leq 1.1 \times 10^4 M_\odot$ ) and  $\mu = 10.04$ ,  $\sigma = 0.65$  ( $\beta \simeq 1.7$  for the best power law fit) for the upper mass range ( $3.6 \times 10^3 \leq M_p \leq 1.35 \times 10^5 M_\odot$ ) (Fig. 2 and table 1). The space density of such clumps falls rapidly inside the inner  $\sim 1.5$ .

Stellar clusters are another class of MPs, which are of minor dynamical significance in this context. About 10 young stellar clusters with masses in the range  $10^2$ – $10^5 M_\odot$  and sizes of order  $R_p \sim 1$  pc were observationally identified (Figer et al. 1999, 2002; Maillard et al. 2004; Figer et al. 2004; Borissova et al. 2005). Again, we fit the lower and upper mass estimates of these clusters (with mass ranges  $3 \times 10^2 - 1.3 \times 10^4 M_\odot$  and  $4.5 \times 10^2 - 7 \times 10^4 M_\odot$ , respectively) with a power-law mass function of a LNPDF, and find  $\beta \simeq 1.3$  and  $\mu \simeq 8.65$ ,  $\sigma = 1.1$  ( $\beta = 1.9$  for the best power law fit; see Fig. 2 and table 1). It is interesting to note in passing that both the GMCs and gas clumps and the clusters have very similar mass functions distributions, but the clusters have a lower mass range, as might be expected if these GMCs are the progenitors of young GC clusters, similar to the relation observed between galactic disk clusters and GMCs (Lada & Lada 2003).

Based on the current observations of the 9 confirmed clusters in the GC, we find that they are dynamically insignificant compared to the GMCs. Note however that their contribution to the relaxation is comparable to that of the stars,

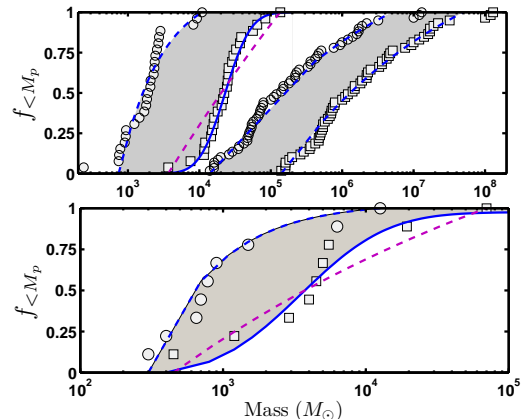


FIG. 2.— Cumulative mass functions of observed massive perturbers in the GC (symbols) with best fit power-law differential distributions,  $dN/dM \propto M^{-\beta}$  (dashed lines) or lognormal distribution with log mean  $\mu$  and log standard deviation  $\sigma$  (solid lines). Top panel: lower (circles) and upper (squares) estimates for the masses of observed molecular clumps (Christopher et al. 2005) (left) and GMCs (Oka et al. 2001) (right) in the GC. The best fit power-law indices for the GMCs are  $\beta_{up} = \beta_{low} = 1.2$  and for the clumps  $\beta_{up} = 1.1$  and  $\beta_{low} = 1.7$ . For the upper estimates of the clumps masses a better fit is found by a log normal distribution with  $\mu = 8.2$ ,  $\sigma = 0.65$ . Bottom panel: likewise for GC clusters (Figer et al. 1999; Figer 2004; Borissova et al. 2005) with  $\beta_{up} = 1.3$  and  $\beta_{low} = 1.9$ , and  $\mu = 10$ ,  $\sigma = 1.1$  for the upper masses estimate.

even when the lower mass estimate is assumed. When the upper mass estimate is assumed, clusters shorten the relaxation time by a factor of 10 (Fig. 1 and table 2). Clusters could play a larger role in relaxation if there are many more yet undiscovered ones in the GC. Based on dynamical simulations, Portegies Zwart et al. (2006) suggest that there may be  $O(100)$  evolved young clusters in the region, undetected against the field stars because of their low surface density. However, Figer et al. (2002) argue that these massive clusters, if they exist, should have been observed. Two young GC cluster candidates were recently discovered by Borissova et al. (2006), one of which may be more massive than  $10^4 M_\odot$ . It is thus possible that the GC harbors some additional undetected massive clusters, although probably not as many as suggested by Portegies Zwart et al. (2006). Such young clusters may grow IMBHs by runaway stellar collisions (e.g. Portegies Zwart et al. 2004; Freitag et al. 2004), which would then sink to the center by dynamical friction, dragging with them the cluster core. Portegies Zwart et al. (2006) estimate that many IMBHs may have migrated to the central 10 pc of GC in this way, however there is as yet no observational evidence supporting this idea.

The MBH's dynamical influence extends up to a radius  $r_h$  containing  $O(M_\bullet)$  mass in stars, which in the GC falls in the range 2–4 pc, depending on the operative definition of  $r_h$  and the uncertainties in the value of  $M_\bullet$  and of the density of the surrounding stellar cluster (see Alexander 2005, sec 3.1.2). Thus most Galactic MPs, and in particular the massive ones, lie outside  $r_h$ . Table (1) summarizes the estimated properties of the observed MPs.

The observed MP species vary in their spatial distributions and mass functions, which are not smooth or regular, and their distribution constantly changes as their orbits decay by dynamical friction and new MPs are formed and destroyed. It is thus likely that the presently observed MPs are but one realization of a much smoother and regular (well-mixed) underlying distribution. Consequently, we construct several simpli-



TABLE 1  
ABUNDANCES OF OBSERVED MASSIVE PERTURBERS IN THE GALACTIC CENTER

MP type	$r^a$ (pc)	$N_p$	$M_p (M_\odot)$	$\beta$	$(\mu, \sigma)$	$\langle M_p^2 \rangle^{1/2} (M_\odot)$	$R_p$ (pc)	References
Observed GMCs	< 100	$\sim 100$	$10^4 - 10^8$	1.2		$3 \times 10^6 - 3 \times 10^7$	5	Oka et al. (2001); Güsten & Philipp (2004)
Observed clusters	< 100	$\sim 10$	$10^2 - 10^5$	1.3	(8.2, 1.1)	$4.8 \times 10^3 - 2.4 \times 10^4$	1	Figer et al. (1999, 2002); Figer (2004) Maillard et al. (2004); Borissova et al. (2005)
Observed clumps	1.5 – 3	$\sim 25$	$10^2 - 10^5$	1.1 – 1.7	(10, 0.65)	$3.7 \times 10^3 - 4.1 \times 10^4$	0.25	Genzel et al. (1985); Christopher et al. (2005)

<sup>a</sup>Projected distance range enclosing observed MPs.

TABLE 2  
MASSIVE PERTURBERS MODELS

Model	$r$ (pc) <sup>a</sup>	$N_p$ <sup>b</sup>	$M_p (M_\odot)$	$\beta$	$\mu, \sigma$
GMC1	5–100	100	$10^5 - 5 \times 10^7$	1.2	–
	1.5–5	30	$3 \times 10^3 - 10^5$	1.1	10.04, 0.65
GMC2	5–100	100	$10^4 - 5 \times 10^6$	1.2	–
	1.5–5	30	$7 \times 10^2 - 10^4$	1.7	–
Clusters1	1.5–100	10	$5 \times 10^2 - 7 \times 10^4$	1.3	–
Clusters2	1.5–100	10	$3 \times 10^2 - 10^4$	1.9	8.16, 1.1
Stars	5–100	$2 \times 10^8$	1	–	–
Stars	1.5–5	$8 \times 10^6$	1	–	–

<sup>a</sup>Distance range enclosing observed MPs.

<sup>b</sup> $N_p(r) \propto r^{-2}$  in the given range is assumed.

<sup>c</sup> $\mu_2^{\text{obs}} = \sum_i \mu_{p,i}^2 / N_* M_*^2$ , where  $M_{p,i}$  is the observed MP's mass.

fied MP models for our numeric calculations (table 2) that are based on the observed properties of the MPs (§4), and our best fits for their mass functions. The simplifications involve the following assumptions. (i) A smooth, spherically symmetric MP number density distribution,  $N_p(r) \propto r^{-2}$  between the cutoffs  $r_{\text{MP}} < r < r_{\text{out}}$  ( $r_{\text{out}}$  does not play an important role, see below), with a random velocity field. (ii) A single or broken power-law MP mass functions,  $dN_p/dM_p \propto M_p^{-\beta}$  (or a lognormal distribution in the appropriate cases). (iii) A single mass stellar population of  $1 M_\odot$  stars with a number density distribution  $N_*(r) \propto r^{-2}$  outside the inner 1.5 pc (i.e. a constant MP to star ratio). (iv) Mutually exclusive perturber types (i.e., a single type of perturber is assumed to dominate relaxation, as indicated by the detailed calculations presented in Fig. 1).

The five MP models are detailed in table 2: Stars, Clusters1, Clusters2, GMC1 and GMC2, represent respectively the case of relaxation by stars only, by heavy and light stellar clusters, and by heavy GMCs and light GMCs. Table 2 lists  $\mu_2$ , the ratio of the 2nd moment of the various MP mass distributions to that of the stars.

#### 4. MASSIVE PERTURBER-DRIVEN INTERACTIONS WITH A MBH

The maximal differential loss-cone refilling rate, which is also the close encounters event rate,  $d\Gamma/dE$ , is reached when relaxation is efficient enough to completely refill the loss cone during one orbit (Eq. 7). Further decrease in the relaxation time does not affect the event rate at that energy. MPs can therefore increase the differential event rate over that predicted by stellar relaxation, only at high enough energies,  $E > E_c$  (equivalently, small enough typical radii,  $r < r_c$ ), where slow stellar relaxation fails to refill the empty loss-cone. The extent of the empty loss-cone region increases with the maximal periapse  $q$ , which in turn depends on the close encounter process of interest. For example, the tidal disruption of an object of mass  $M$  and size  $R$  occurs when  $q < r_t$ ,

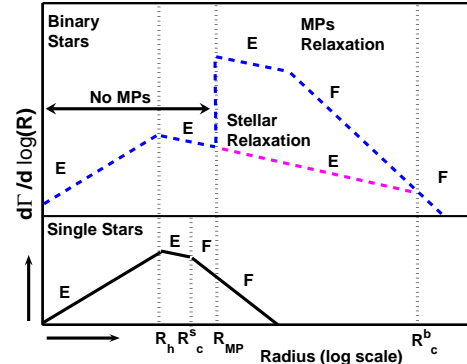


FIG. 3.— A schematic representation of the local contribution to the tidal disruption rate for a single component MP model (e.g. GMC2 without the central clumps, so that  $r_{\text{MP}} = 5$  pc). Top: the disruption rate of binaries (a constant binary fraction is assumed here for simplicity) due to stellar relaxation (bottom dashed line) and MPs (top dashed line). Bottom: the disruption rate of single stars for both perturber models. Empty and full loss-cone regimes are denoted by “E” and “F”, respectively. The initial orbital energy of the disrupted objects is expressed by the corresponding radius of a circular orbit,  $r$ . For  $r < r_h$ , stellar density and velocity distributions of  $N_*(r) \propto r^{-3/2}$  and  $\sigma(r) \propto r^{-1/2}$  are assumed; for  $r > r_h$ ,  $N_*(r) \propto r^{-2}$  and  $\sigma(r) = \text{const}$ . The transition from the empty to full loss-cone regime (for stellar relaxation) occurs at the critical radius  $r_c^s < r_{\text{MP}}$  for single stars and at  $r_c^b \gg r_{\text{MP}}$  for binaries.

the tidal disruption radius,

$$r_t \simeq R (M_\bullet / M)^{1/3}. \quad (16)$$

This approximate disruption criterion applies both for single stars ( $M = M_*$ ,  $R = R_*$ ) and for binaries, where  $M$  is the combined mass of the binary components and  $R$  is the binary’s semi-major axis,  $a$ . Stellar radii are usually much smaller than typical binary separations, but stellar masses are only  $\sim 2$  times smaller than binary masses. Binaries are therefore disrupted on larger scales than single stars. In the GC this translates to an empty (stellar relaxation) loss-cone region extending out to  $r_c^s \sim 3$  pc for single stars and out to  $r_c^b > 100$  pc for binaries. In the GC  $r_{\text{MP}} \lesssim r_c^s \ll r_c^b$ , and so MPs are expected to increase the binary disruption rate by orders of magnitude, but increase the single star disruption rate only by a small factor. This is depicted qualitatively in figure (3), which shows the local rates ( $d\Gamma/d \log r$ ) for disruption of single stars and binaries due to stellar relaxation or relaxation by a simplified one component MP model.

Figure (3) also shows that the MP-induced disruption rate is dominated by binaries originating near the inner cutoff  $r_{\text{MP}}$  (in the following discussion the initial orbital energy of the disrupted objects is expressed by the corresponding radius of a circular orbit,  $r \sim GM(<r)/2E$ ). This is qualitatively different from the usual case of stellar tidal disruption induced by stellar relaxation, which mainly occurs inside  $r_c^s$  and is dom-

inated by stars originating near the *outer* limit  $\min(r_c^s, r_h)$ ; usually  $r_c^s \sim r_h$  (Lightman & Shapiro 1977). The difference can be understood by considering the  $r$ -dependence of  $d\Gamma/d\log r$ . Neglecting logarithmic terms, the empty and full local loss-cone rates are, respectively (Eqs. 5, 6)

$$\frac{d\Gamma_e}{d\log r} \sim \frac{N_*(<r)}{t_r(r)}, \quad (17)$$

$$\frac{d\Gamma_f}{d\log r} \sim \left[ \frac{M_\bullet}{M_\bullet + M_*(<r)} \right] \left( \frac{q}{r} \right) \frac{N_*(<r)}{P(r)}, \quad (18)$$

where  $N_*(<r)$  is the number of stars enclosed within  $r$ .

Inside  $r_h$ , the potential is dominated by the MBH ( $M_*(<r)/M_\bullet \ll 1$ ),  $N_* \propto r^{-\alpha_1}$  with  $\alpha_1 < 2$  for most dynamical scenarios (e.g. Bahcall & Wolf 1977; Young 1980) and the velocity dispersion is Keplerian,  $\sigma \propto r^{-1/2}$ . The orbital period scales as  $P \propto r^{3/2}$  and  $t_r \sim (M_\bullet/M_*)^2 P / [(\log N_*)N_*]$ . The local disruption rates are then  $d\Gamma_e/d\log r|_{r<r_h} \propto r^{9/2-2\alpha_1}$  and  $d\Gamma_f/d\log r|_{r<r_h} \propto r^{1/2-\alpha_1}$ . For plausible values of  $1/2 < \alpha_1 < 9/4$ ,  $\Gamma_e$  increases with  $r$  whereas  $\Gamma_f$  decreases with  $r$ , so the rate is dominated by stars near  $r_c$  (Lightman & Shapiro 1977). Outside  $r_h$ , the stellar distribution is usually assumed to be near isothermal,  $N_* \propto r^{-\alpha_2}$  with  $\alpha_2 \sim 2$  and a velocity dispersion  $\sigma \sim \text{const}$ , and the potential is dominated by the stars ( $M_\bullet \ll M_*(<r) \propto r^{3-\alpha_2}$ ). The orbital period scales as  $P \propto r^{\alpha_2/2}$  and  $t_r \sim N_* P / \log N_*$ . The local disruption rates are then  $d\Gamma_e/d\log r|_{r>r_h} \propto r^{-\alpha_2/2} \sim r^{-1}$  and  $d\Gamma_f/d\log r|_{r>r_h} \propto r^{-1-\alpha_2/2} \sim r^{-2}$ . For  $\alpha_2 \sim 2$  both rates increase toward small radii. Since for most Galactic MP types  $r_{\text{MP}} > r_h$ , the disruption rate is dominated by stars near  $r_{\text{MP}}$ . For example, when the loss-cone is empty,  $\sim 50\%$  of the total rate is due to MPs at  $r < 2r_{\text{MP}}$ ; when the loss-cone is full,  $\sim 75\%$  of the total rate is due to MPs at  $r < 2r_{\text{MP}}$ .

#### 4.1. Interactions with single stars

GMCs, gas clumps and clusters in the GC are abundant only beyond the central  $r_{\text{MP}} \sim 1.5$  pc, whereas the empty loss-cone regime for tidal disruption of single stars extends only out to  $r_c^s \sim 3$  pc. For inspiral processes such as GW emission,  $r_c$  is  $\sim 100$  times smaller still (Hopman & Alexander 2005, 2006b). The effect of such MPs on close encounter events involving single stars is thus suppressed (weaker tidal effects by MPs at  $r > r_c^s$  are not considered here). This is contrary to the suggestion of Zhao et al. (2002), who assumed that the effect of MPs fully extends to the empty loss-cone regime. We find that the enhancement of MPs over stellar relaxation to the single stars disruption rate is small, less than a factor of 3, and is due to stars scattered by gas clumps in the small empty-loss cone region between  $r_{\text{MP}} \sim 1.5$  pc and  $r_c^s \sim 3$  pc. A possible exception to this conclusion is the hypothesized population of IMBHs (Portegies Zwart et al. 2006), not modeled here, whose distribution could extend to the inner pc (e.g. the IMBH candidate in IRS 13, Maillard et al. 2004, but see Schödel et al. 2005 and Paumard et al. 2006).

#### 4.2. Interactions with stellar binaries

The empty loss cone region for binary-MBH interactions extends out to  $> 100$  pc because of their large tidal radius. On these large scales MPs are abundant enough to dominate the relaxation processes. Here we focus on 3-body exchange interactions (Hills 1991, 1992; Yu & Tremaine 2003), which lead to the disruption of the binary, the energetic ejection of

one star, and the capture of the other star on a close orbit around the MBH.

Various phenomena associated with such exchange interactions were suggested and explored. Hills (1988) and later Yu & Tremaine (2003), Gualandris et al. (2005), Ginsburg & Loeb (2006) and Bromley et al. (2006), studied hyper-velocity stars ejected from the GC following tidal disruption by the MBH. Gould & Quillen (2003) suggested this mechanism to explain the origin of the young stars near the Galactic MBH. Miller et al. (2005) proposed that compact objects captured following a binary disruption event will eventually be sources of GWs from zero-eccentricity orbits, in contrast to high-eccentricity sources typical of single star inspiral (Hopman & Alexander 2005).

The event rates estimated by these authors vary substantially. Hills (1988) assumed a full loss-cone and a fraction  $f_{\text{bin}} = 0.02$  of the stars in binaries with small enough semi-major axis to produce a high-velocity star ( $a < 0.1$  AU), and derived a 3-body exchange rate of  $\sim 10^{-3}(f_{\text{bin}}/0.02) \text{ yr}^{-1}$ . Yu & Tremaine (2003) took into account the empty loss cone regime, and argued for a higher fraction of relevant binaries ( $f_{\text{bin}} = 0.04$  for binaries with  $a < 0.3$  AU that can survive 0.8 pc from the MBH), thereby obtaining a rate of  $\sim 2.5 \times 10^{-6}(f_{\text{bin}}/0.04) \text{ yr}^{-1}$ , 3 orders of magnitude smaller than that estimated by Hills. These calculations assumed the same binary separation for all binaries and a constant binary fraction at all distances from the MBH (two possibilities were considered,  $a = 0.3$  AU and  $a = 0.03$  AU).

The binary fraction and typical binary semi-major axis depend on the binary mass, and on the rate at which binaries evaporate by encounters with other stars. This depends in turn on the stellar densities and velocities, and therefore on the distance from the MBH. Here we take these factors into account and estimate in detail the 3-body exchange rate for MP-driven relaxation. The rate is proportional to the binary fraction in the population, which is the product of the poorly-known binary IMF in the GC and the survival probability against binary evaporation.

We assume for simplicity equal mass binaries,  $M_{\text{bin}} = 2M_*$ , since the observations indicate that moderate mass ratios dominate the binary population (Duquennoy & Mayor 1991; Kobulnicky et al. 2006). The evaporation timescale at distance  $r$  from the center for a binary of semi-major axis  $a$  composed of two equal mass stars of mass  $M_*$  and lifetime  $t_*$  is (e.g. Binney & Tremaine 1987)

$$t_{\text{evap}}(M_*, a, r) = \frac{M_{\text{bin}}}{\langle M_* \rangle} \frac{\sigma(r)}{16\sqrt{\pi}\rho(r)Ga \ln \Lambda_{\text{bin}}}. \quad (19)$$

The Coulomb factor for binary evaporation,  $\Lambda_{\text{bin}} = a\sigma^2/4G\langle M_* \rangle$ , expresses the fact that the binary is only affected by close perturbations at distances smaller than  $\sim a/2$ . The MPs considered here are extended objects (table 2) and therefore do not affect the binary evaporation timescale (IMBH MPs could be a possible exception). Although binary evaporation is a stochastic process and the actual time to evaporation differs from binary to binary, we expect a small scatter in the evaporation rate,  $\Delta t_{\text{evap}}^{-1}/t_{\text{evap}}^{-1} \ll 1$ , because evaporation is a gradual process caused by numerous weak encounters. Evaporation is thus better approximated as a fixed limit on the binary lifetime, rather than as a Poisson process (where  $\Delta t_{\text{evap}}^{-1}/t_{\text{evap}}^{-1} = 1$ ). The maximal binary lifetime is then  $\tau = \min([t_H, t_*(M_*), t_{\text{evap}}(M_*, a, r)])$ , where  $t_H$  is the Hubble time, taken here to be the age of the Galaxy. It is well established that the central 100–200 pc of

the GC have undergone continuous star formation over the lifetime of the Galaxy (Serabyn & Morris 1996; Figer et al. 2004). Assuming a constant star formation rate over time  $t_H$ , the differential binary distribution at time  $t$  is  $dN_{\text{bin}}/da|_t = f_{\text{bin}} df/da|_0 \Gamma_* \min(t, \tau)$ , where  $df/da|_0$  is the normalized initial semi-major axis distribution, which can be observed in binaries in low-density environments where  $t_{\text{evap}} \rightarrow \infty$ , and  $\Gamma_*$  is the single star formation rate, which is normalized to the observed present day stellar density by setting  $t = t_H$  and taking  $t_{\text{evap}} \rightarrow \infty$  for singles, so that  $\Gamma_* = N_*/\min(t_H, t_*)$ . The present-day binary semi-major axis distribution is therefore

$$\frac{dN_{\text{bin}}}{da} \Big|_{t_H} = f_{\text{bin}}(M_*) \frac{df}{da} \Big|_0 N_*(r) \times \min \left\{ 1, \frac{t_{\text{evap}}(M_*, a, r)}{\min[t_H, t_*(M_*)]} \right\}. \quad (20)$$

The capture probability and the semi-major axis distribution of captured stars were estimated by simulations (Hills 1991, 1992; Yu & Tremaine 2003). Numeric experiments indicate that between 0.5–1.0 of the binaries that approach the MBH within the tidal radius  $r_t(a)$  (Eq. 16) are disrupted. Here we adopt a disruption efficiency of 0.75. The harmonic mean semi-major axis for 3-body exchanges with equal mass binaries was found to be (Hills 1991)

$$\langle a_1 \rangle \simeq 0.56 \left( \frac{M_\bullet}{M_{\text{bin}}} \right)^{2/3} a \simeq 0.56 \left( \frac{M_\bullet}{M_{\text{bin}}} \right)^{1/3} r_t, \quad (21)$$

where  $a$  is the semi-major axis of the infalling binary and  $a_1$  that of the captured star (the MBH-star “binary”). Most values of  $a_1$  fall within a factor 2 of the mean. This relation maps the semi-major axis distribution of the infalling binaries to that of the captured stars: the harder the binaries, the more tightly bound the captured stars. The velocity at infinity of the ejected star (neglecting the Galactic potential) is  $v_{\text{BH}}^2 = 2^{1/2} (GM_{\text{bin}}/a) (M_\bullet/M_{\text{bin}})^{1/3} \propto M_{\text{bin}}^{2/3}/a$  (an equal mass binary with periape at  $r_t$  is assumed; Hills 1988). The harder the binary, the higher is  $v_{\text{BH}}$ . The periape of the captured star is at  $r_t$ , and therefore its eccentricity is very high (Hills 1991, 1992; Miller et al. 2005),  $e = 1 - r_t/a_1 \simeq 1 - 1.8(M_{\text{bin}}/M_\bullet)^{1/3} \gtrsim 0.98$  for values typical of the GC.

We now consider separately the implications of 3-body exchange interactions of the MBH with old ( $t_* \gtrsim t_H$ ) binaries and massive young ( $t_* < 5 \times 10^7$  yr) binaries.

#### 4.2.1. Low mass binaries

The properties of binaries in the inner GC are at present poorly determined. The period distribution of Solar neighborhood binaries can be approximated by a log normal distribution with a median period of 180 years ( $a \sim 40$  AU) (Duquennoy & Mayor 1991). The total binary fraction of these binaries is estimated at  $f_{\text{bin}} \sim 0.3$  (Lada 2006). Adopting these values for the GC, the total binary disruption rate by the MBH can then be calculated, as described in §2, by integrating  $dN_{\text{bin}}/da$  (Eqs. 20) over the binary  $a$  distribution and over the power-law stellar density distribution of the GC up to 100 pc (Genzel et al. 2003). Table (3) lists the capture rates for the different perturber models, assuming a typical old equal-mass binary of  $M_{\text{bin}} = 2 M_\odot$ .

The old, low-mass binary disruption rate we derive for stellar relaxation alone is  $\sim 5 \times 10^{-7} \text{ yr}^{-1}$ ,  $\sim 5$  times lower, but still in broad agreement with the result of Yu & Tremaine

(2003). Their rate is somewhat higher because they assumed a constant binary fraction and a constant semi-major axis for all binaries, even close to the MBH, where these assumptions no longer hold.

MPs increase the binary disruption and high-velocity star ejection rates by factors of  $\sim 10^{1-3}$  and effectively accelerate stellar migration to the center. This can modify the stellar distribution close to the MBH by introducing a “source term” to the stellar current into the MBH. Low-mass stars are at present too faint to be directly observed in the GC. However, such a source term may have observable consequences since it can increase the event rate of single star processes such as tidal disruption, tidal heating and GW emission from compact objects, in particular from compact objects on zero-eccentricity orbits (Miller et al. 2005) (in contrast, GW from inspiraling single stars occur on high-eccentricity orbits, Hopman & Alexander 2005). We calculated numerical solutions of the Fokker-Planck equation for the stellar distribution around the MBH with a captured stars source term. These preliminary investigations (Perets, Hopman & Alexander, in prep.) confirm that the total accumulated mass of captured stars does not exceed the dynamical constraints on the extended mass around the MBH (Mouawad et al. 2005), because 2-body relaxation and likely also resonant relaxation (Rauch & Tremaine 1996; Hopman & Alexander 2006a) scatters enough of them into the MBH or to wider orbits.

#### 4.2.2. Young massive binaries

MPs may be implicated in the puzzling presence of a cluster of main sequence B-stars ( $4 \lesssim M_* \lesssim 15 M_\odot$ ) in the inner  $\sim 1''$  ( $\sim 0.04$  pc) of the GC. This so-called “S-cluster” is spatially, kinematically and spectroscopically distinct from the young, more massive stars observed farther out, on the  $\sim 0.05$ – $0.5$  pc scale, which are thought to have formed from the gravitational fragmentation of one or two gas disks (Levin & Beloborodov 2003; Genzel et al. 2003; Milosavljević & Loeb 2004; Paumard et al. 2006). There is however still no satisfactory explanation for the existence of the seemingly normal, young massive main sequence stars of the S-cluster, so close to a MBH (see review of proposed models by Alexander 2005; also a recent model by Levin 2006).

Here we revisit an idea proposed by Gould & Quillen (2003), that the S-stars were captured near the MBH by 3-body exchange interactions with infalling massive binaries. Originally, this exchange scenario lacked a plausible source for the massive binaries. Gould & Quillen speculated that they originated in an unusually dense and massive young cluster on an almost radial infall trajectory, but concluded that such a finely-tuned scenario seems unlikely. Furthermore, a massive cluster is expected to leave a tidally stripped tail of massive stars beyond the central 0.5 pc (Kim et al. 2004; Gürkan & Rasio 2005), which are not observed (Paumard et al. 2006). Alternatively, it must contain an unusually massive central IMBH to hold it together against the tidal field of the GC (Hansen & Milosavljević 2003). However, such a massive IMBH is well beyond what is predicted by simulations of IMBH formation by runaway collisions (Gürkan et al. 2004; Gürkan & Rasio 2005), or anticipated by extrapolating the  $M/\sigma$  relation (Ferrarese & Merritt 2000; Gebhardt et al. 2000) to clusters.



TABLE 3  
TOTAL BINARY DISRUPTION RATE AND NUMBER OF CAPTURED YOUNG STARS

Model	Disruption rate (yr <sup>-1</sup> )		Young Stars <sup>a</sup>		Young HVSS <sup>b</sup>
	$r < 0.04$ pc	$r < 0.4$ pc	$r < 0.04$ pc	$0.04 < r < 0.4$ pc	
GMC1	$1.1 \times 10^{-4}$	$3.2 \times 10^{-4}$	39.4	5.2	342
GMC2	$2.8 \times 10^{-5}$	$1.8 \times 10^{-4}$	6	1.4	49
Clusters1	$6.4 \times 10^{-7}$	$9.7 \times 10^{-7}$	0.19	0.004	1.9
Clusters2	$2.6 \times 10^{-8}$	$4 \times 10^{-8}$	0.01	$10^{-4}$	0.1
Stars	$3.4 \times 10^{-7}$	$5.3 \times 10^{-7}$	0.15	0.003	1.3
Observed	?	?	$10 - 35^c$	?	$43 \pm 31^d$

<sup>a</sup>Main sequence B stars with lifespan  $t < 5 \times 10^7$  yr.

<sup>b</sup>Main sequence B stars with lifespan  $t < 4 \times 10^8$  yr. Notice that only 20 percents of these ejected stars could be observed in regions covered by current surveys.

<sup>c</sup> $\sim 10$  stars with derived  $a \lesssim 0.04$  pc.  $\gtrsim 30$  stars are observed in the area.

<sup>d</sup>Estimated from the observed 5 HVSSs, at distances between 20-120 pc from the GC (Brown et al. 2006a)

MP-driven 3-body exchanges circumvent the problems of the cluster infall scenario by directly bringing massive *field* binaries to  $r_t$ , without requiring massive clusters of unusual, perhaps even impossible properties. The ongoing star formation in the central  $\sim 100$  pc implies the presence of a large reservoir of massive stars there, which are indeed observed in the central few  $\times 10$  pc both in dense clusters and in the field (Figer et al. 1999; Figer 2003; Munro et al. 2006). It is plausible that a high fraction of them are in binaries.

We model the binary population of the GC in the S-stars mass range,  $4 \lesssim M_* \lesssim 15 M_\odot$ , by assuming equal mass binaries that follow the single star mass function with an initial binary fraction of  $f_{\text{bin}} \sim 0.75$ , as observed elsewhere in the Galaxy (Lada 2006; Kobulnicky et al. 2006). Because the stellar evolutionary lifespan of such stars is relatively short, massive binaries are essentially unaffected by dynamical evaporation. We assume star formation at a constant rate for 10 Gyr with a Miller-Scalo IMF (Miller & Scalo 1979), and use a stellar population synthesis code (Sternberg et al. 2003) with the Geneva stellar evolution tracks (Schaller et al. 1992) to estimate that the present day number fraction of stars in the S-star mass range is  $3.5 \times 10^{-4}$  (and less than 0.01 of that for  $M_* > 15 M_\odot$  stars). Note that if star formation in the GC is biased toward massive stars (Figer 2003; Stolte et al. 2005), this estimate should be revised upward. We adopt the observed Solar neighborhood distribution of the semi-major axis of massive binaries, which is log-normal with  $\langle \log a \rangle = -0.7 \pm 0.6$  AU (i.e. 63% of the binaries with  $a = 0.2_{-0.15}^{+0.60}$  AU; 91% with  $a = 0.2_{-0.19}^{+2.96}$  AU) (Garmany et al. 1980; Kobulnicky et al. 2006). Massive binaries are thus typically harder than low-mass binaries, and will be tidally disrupted (Eq. 16) closer to the MBH and leave a more tightly bound captured star.

We represent the massive binaries by one with equal mass stars in the mid-range of the S-stars masses, with  $M_{\text{bin}} = 15 M_\odot$  and  $t_*(7.5 M_\odot) \simeq 5 \times 10^7$  yr, and integrate over the stellar distribution and the binary  $a$  distribution as before, to obtain the rate of binary disruptions,  $\Gamma$ , the mean number of captured massive stars in steady state,  $N_* = \Gamma t_*$ , and their semi-major axis distribution (Eq. 21). Table (3) compares the number of captured young stars in steady state, for the different MP models, on the  $r < 0.04$  pc scale (the S-cluster) and  $0.04 < r < 0.4$  pc scale (the stellar rings) with current observations (Eisenhauer et al. 2005; Paumard et al. 2006).

The S-stars are found in the central  $< 0.04$  pc (Ghez et al. 2005; Eisenhauer et al. 2005). If they were captured by binary disruptions, they must have originated from massive bi-

naries with  $a \lesssim 3.5$  AU. This is consistent with semi-major axis distribution of massive binaries. The number of captured massive stars falls rapidly beyond 0.04 pc (table 3) because wide massive binaries are rare. This capture model thus provides a natural explanation for the central concentration of the S-cluster (Fig 4). The absence of more massive stars in the S-cluster ( $M_* > 15 M_\odot$ , spectral type O V) is a statistical reflection of their much smaller fraction in the binary population. Figure (4) and table (3) compare the cumulative semi-major axis distribution of captured B-stars, as predicted by the different MP models, with the total number of young stars observed in the inner 0.04 pc ( $\sim 35$  stars, Eisenhauer et al. 2005; Ghez et al. 2005; Paumard et al. 2006). Of these, only  $\sim 10$  have full orbital solutions (in particular  $a$  and  $e$ ) at present. For the others we assume the *ansatz* that  $a$  is similar to the observed projected position. The numbers predicted by the GMC-dominated MP models are consistent with the observations, unlike the stellar relaxation model that falls short by two orders of magnitude.

The binary capture model predicts that captured stars have very high initial eccentricities. Most of the solved S-star orbits do have  $e > 0.9$ , but a couple have  $e \sim 0.3 - 0.4$  (Eisenhauer et al. 2005). Normal, non-coherent stellar relaxation is slow, even after taking into account the decrease in  $t_r$  toward the center due to mass segregation (Hopman & Alexander 2006b). It is unlikely that it could have decreased the eccentricity of these stars over their relatively short lifetimes. However, the much faster process of resonant relaxation (Rauch & Tremaine 1996) may be efficient enough to randomize the eccentricity of a fraction of the stars, and could thus possibly explain the much larger observed spread in eccentricities (Hopman & Alexander 2006a). Additional orbital solutions and a better estimate of the efficiency of resonant relaxation in the GC are required for more detailed comparisons between observations and the MP model predictions.

#### 4.2.3. Hyper-velocity stars

Each captured star is associated with an ejected companion, which in some cases is launched with a very high velocity. The one-to-one correspondence between the number of captured S-stars and the number of early-type hyper-velocity stars (HVSSs) is thus a generic prediction of binary capture models. The MP capture scenario specifically implies the continuous and isotropic ejection of both young and old HVSSs from the GC. Recent observations of HVSSs (Brown et al. 2005; Hirsch et al. 2005; Edelmann et al. 2005; Brown et al. 2006a,b) are consistent with a GC origin and fa-

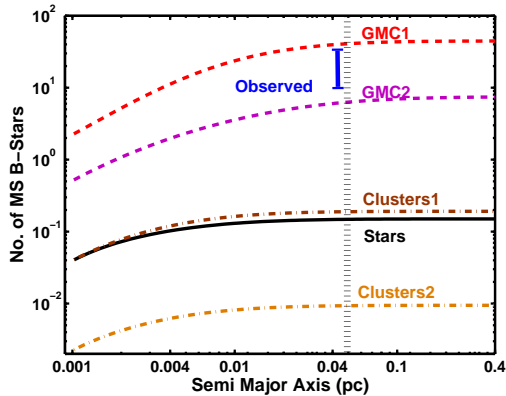


FIG. 4.— Cumulative number of young B-stars in the GC as predicted by the MP models and by stellar two-body relaxation (listed in table 2). The vertical bar represents the total number of observed young stars inside 0.04 pc (Eisenhauer et al. 2005; S. Gillessen, priv. comm.). The dotted vertical line marks the approximate maximal distance in which captured B-stars are expected to exist.

vor a steady state temporal distribution and an isotropic spatial distribution over a burst-like non-spherical distribution that is expected for HVSs triggered by the infall of a cluster (Levin 2005; Haardt et al. 2006; Baumgardt et al. 2006).

Two of the recently observed HVSs ( $v \sim 560\text{--}710 \text{ km s}^{-1}$ , Brown et al. 2005, 2006a; Fuentes et al. 2006; Edelmann et al. 2005; Brown et al. 2006b) were spectrally identified as late B V young massive stars (masses of  $3\text{--}5 M_{\odot}$ , MS lifespans of  $(1\text{--}4) \times 10^8 \text{ yr}$  and number fraction  $\sim 10^{-3}$  in the population), implying a total population of  $43 \pm 31$  such hyper-velocity stars in the Galaxy (Brown et al. 2006a). We model the parent binaries of these HVSs by equal mass binaries of  $M_{\text{bin}} = 8 M_{\odot}$  and  $t_{*}(4M_{\odot}) = 2 \times 10^8 \text{ yr}$ . The ejection velocity was found in numerical simulations (Hills 1988; Bromley et al. 2006) to scale as

$$v_{\text{BH}} = 1776 \text{ km s}^{-1} \times \left( \frac{a}{0.1 \text{ AU}} \right)^{-1/2} \left( \frac{M_{\text{bin}}}{2M_{\odot}} \right)^{1/3} \left( \frac{M_{\text{BH}}}{3.7 \times 10^6 M_{\odot}} \right)^{1/6} \quad (22)$$

To reproduce the high HVS velocities we consider binaries with  $a < 1 \text{ AU}$ , which are tidally disrupted at  $r_t < 3.7 \times 10^{-4} \text{ pc}$  and eject a HVS with  $v_{\text{BH}} \gtrsim 900 \text{ km s}^{-1}$ , the escape velocity from the bulge (Haardt et al. 2006). Taking only the GMCs into account, we predict that tens to hundreds such HVSs exist in the Galaxy, in agreement with the deduced HVS populations, whereas stellar relaxation predicts only 1.3 such stars (see table 3).

We note Brown et al. (2006a) used the  $10^{-5} \text{ yr}^{-1}$  total rate of hyper-velocity star ejection calculated by Yu & Tremaine (2003) (including binaries of all stellar types, assuming stellar relaxation only and normalized to a fiducial 10% binary fraction) to estimate the number of late B V HVSs in a Salpeter IMF at 10–25. This theoretical prediction seems in rough agreement with the observations (and contradicts our much lower estimate of 1.3 HVSs). However, the rates of Yu & Tremaine are inapplicable here and lead to a significant overestimate of the number of HVSs because their binary population model is not appropriate for massive binaries in the GC. On the one hand, the young binary population does not extend all the way to the center, as assumed by Yu & Tremaine for the general binary population (Following Paumard et al. 2006

who do not find any B V stars between 0.5–1 pc of the GC, we truncate the massive binary population inside 1.5 pc). The massive binary population in the GC is  $\text{few} \times 10$  times smaller than implied by a simple scaling of the Yu & Tremaine general binary population. On the other hand, the binary fraction of young massive binaries is 70% rather than 10% (§4.2.2). We conclude that the agreement found by Brown et al. is accidental, and that binary disruption by stellar relaxation is insufficient to explain the number of observed HVSs, whereas MP-induced relaxation can reproduce the observations.

## 5. SUMMARY

Relaxation by MPs dominates relaxation by 2-body stellar interactions when the ratio between the 2nd moments of their respective mass functions satisfies  $\mu_2 = N_p \langle M_p^2 \rangle / N_* \langle M_*^2 \rangle \gg 1$ . We show that Galactic MPs (stellar clusters, GMCs and smaller molecular gas clumps that exist outside the inner few pc) dominate and accelerate relaxation in the inner  $\sim 100 \text{ pc}$  of the GC. This is plausibly the case in the centers of late-type galaxies in general. There is also evidence for molecular gas in the centers of late-type galaxies (e.g. Rupen 1997; Knapp 1999), which suggests that MPs may dominate relaxation there as well, and lead to the relaxation of the central regions of galactic bulges in general.

Relaxation determines the rate at which stars and binaries are deflected to near radial (loss-cone) orbits that bring them closer to the MBH than some critical periastron  $q$ , where they undergo a strong destructive interaction with it. The size of  $q$  depends on the nature of the interaction of interest (e.g. tidal disruption, 3-body exchange). It is much larger for binaries than for single stars due to the binary’s larger effective size.

We extend loss-cone theory to approximately treat rare encounters with MPs, and apply it to explore the implications of MPs on the rates of different types of close encounters. The rate reaches its maximum when loss-cone orbits are replenished by scattering within an orbital time (the full loss-cone regime). This is more easily achieved when the phase-space volume of the loss-cone is small, that is, when  $q$  is small. MPs thus affect only those processes with large  $q$  whose loss-cone is too large to be efficiently replenished by stellar encounters (the empty loss-cone regime).

We show that MPs will not contribute much to the disruption of single stars in the GC, whose loss-cone is efficiently replenished by stars outside the central  $\sim 2 \text{ pc}$  (MPs may accelerate the consumption of stars by more massive MBHs, where  $q$  is significantly larger, or the capture of stars in accretion disks). However, MPs will enhance by factors of 10–1000 the tidal disruption rate of infalling binaries, which result in the capture of one of the stars on a tight orbit around the MBH, and the ejection at high velocity of the other star (Hills 1991, 1992; Yu & Tremaine 2003). The enhancement of the event rates is dominated by the innermost MPs, and so the uncertainty in the MP distribution on the smallest scales dominates the uncertainties in the total event rate. Detailed observations of MPs in the inner GC allow us to robustly predict their effects in the Galaxy. We show that MP-induced disruptions of relatively rare massive binaries can naturally explain the puzzling presence of normal-appearing main sequence B stars in the central 0.04 pc of the GC (Eisenhauer et al. 2005), and at the same time can account for the observed HVSs well on their way out of the Galaxy (Brown et al. 2005; Edelmann et al. 2005; Hirsch et al. 2005; Brown et al. 2006a,b; Bromley et al. 2006). Tidal disruptions of the many more faint low-mass binaries can efficiently sup-

ply single stars on very eccentric tight orbits near the MBH. Such an increase in the numbers of stars in tight orbit near the MBH may increase the rates of single star processes such as tidal disruption and heating or GW emission from tightly bound compact objects (Miller et al. 2005).

Finally, MP-induced interactions also have cosmological implications for the coalescence of binary MBHs following galactic mergers (Zhao et al. 2002). We suggest that MPs can accelerate the dynamical decay of binary MBHs by efficiently supplying stars for the slingshot mechanism, and thereby help solve the “last parsec” stalling problem. MP-driven loss-cone

refilling will operate even in the case of a spherical potential, where other suggested mechanisms are inefficient, thus allowing MBHs to coalesce on the dynamical timescale of the galactic merger. A detailed treatment of this idea will be presented elsewhere (Perets & Alexander, in prep.).

TA is supported by ISF grant 295/02-1, Minerva grant 8563 and a New Faculty grant by Sir H. Djangoly, CBE, of London, UK. We are grateful to M. Tsuboi for help in interpreting the giant molecular cloud data.

## REFERENCES

- Alexander, T. 2005, *Phys. Rep.*, 419, 65  
 Alexander, T. & Hopman, C. 2003, *ApJ*, 590, L29  
 Alexander, T. & Livio, M. 2001, *ApJ*, 560, L143  
 —. 2004, *ApJ*, 606, L21  
 Alexander, T. & Morris, M. 2003, *ApJ*, 590, L25  
 Bahcall, J. N. & Wolf, R. A. 1976, *ApJ*, 209, 214  
 —. 1977, *ApJ*, 216, 883  
 Bailey, M. E. 1983, *MNRAS*, 204, 603  
 Baumgardt, H., Gualandris, A., & Portegies Zwart, S. 2006, *ArXiv Astrophysics e-prints*  
 Berczik, P., Merritt, D., & Spurzem, R. 2005, available at <http://xxx.lanl.gov/abs/astro-ph/0507260>  
 Berczik, P., Merritt, D., Spurzem, R., & Bischof, H.-P. 2006, *ApJ*, 642, L21  
 Binney, J. & Tremaine, S. 1987, *Galactic Dynamics* (Princeton, NJ: Princeton University Press)  
 Borissova, J., Ivanov, V. D., Minniti, D., & Geisler, D. 2006, *ArXiv Astrophysics e-prints*  
 Borissova, J., Ivanov, V. D., Minniti, D., Geisler, D., & Stephens, A. W. 2005, *A&A*, 435, 95  
 Bromley, B. C., Kenyon, S. J., Geller, M. J., Barcikowski, E., Brown, W. R., & Kurtz, M. J. 2006, *ArXiv Astrophysics e-prints*  
 Brown, W. R., Geller, M. J., Kenyon, S. J., & Kurtz, M. J. 2005, *ApJ*, 622, L33  
 —. 2006a, *ApJ*, 640, L35  
 —. 2006b, *ApJ*, 647, 303  
 Christopher, M. H., Scoville, N. Z., Stolovy, S. R., & Yun, M. S. 2005, *ApJ*, 622, 346  
 Cohn, H. & Kulsrud, R. M. 1978, *ApJ*, 226, 1087  
 Duquennoy, A. & Mayor, M. 1991, *A&A*, 248, 485  
 Edelmann, H., Napiwotzki, R., Heber, U., Christlieb, N., & Reimers, D. 2005, *ApJ*, 634, L181  
 Eisenhauer, F. et al. 2005, *ApJ*, 628, 246  
 Ferrarese, L. & Merritt, D. 2000, *ApJ*, 539, L9  
 Figer, D. F. 2003, *Astronomische Nachrichten Supplement*, 324, 255  
 Figer, D. F. 2004, in *ASP Conf. Ser. 322: The Formation and Evolution of Massive Young Star Clusters*, ed. H. J. G. L. M. Lamers, L. J. Smith, & A. Nota, 49–+  
 Figer, D. F., Kim, S. S., Morris, M., Serabyn, E., Rich, R. M., & McLean, I. S. 1999, *ApJ*, 525, 750  
 Figer, D. F., Najarro, F., Gilmore, D., Morris, M., Kim, S. S., Serabyn, E., McLean, I. S., Gilbert, A. M., Graham, J. R., Larkin, J. E., Levenson, N. A., & Teplitz, H. I. 2002, *ApJ*, 581, 258  
 Figer, D. F., Rich, R. M., Kim, S. S., Morris, M., & Serabyn, E. 2004, *ApJ*, 601, 319  
 Frank, J. & Rees, M. J. 1976, *MNRAS*, 176, 633  
 Freitag, M., Gürkan, M. A., & Rasio, F. A. 2004, in *ASP Conf. Ser. Vol. 30: Massive Stars in Interacting Binaries*, ed. N. St-Louis & A. Moffat, available at <http://xxx.lanl.gov/abs/astro-ph/0410327>  
 Fuentes, C. I., Stanek, K. Z., Gaudi, B. S., McLeod, B. A., Bogdanov, S., Hartman, J. D., Hickox, R. C., & Holman, M. J. 2006, *ApJ*, 636, L37  
 Garmany, C. D., Conti, P. S., & Massey, P. 1980, *ApJ*, 242, 1063  
 Gebhardt, K. et al. 2000, *ApJ*, 539, L13  
 —. 2003, *ApJ*, 583, 92  
 Genzel, R., Crawford, M. K., Townes, C. H., & Watson, D. M. 1985, *ApJ*, 297, 766  
 Genzel, R. et al. 2003, *ApJ*, 594, 812  
 Gerhard, O. E. & Binney, J. 1985, *MNRAS*, 216, 467  
 Ghez, A. M., Salim, S., Hornstein, S. D., Tanner, A., Lu, J. R., Morris, M., Becklin, E. E., & Duchêne, G. 2005, *ApJ*, 620, 744  
 Ginsburg, I. & Loeb, A. 2006, *MNRAS*, 368, 221  
 Gould, A. & Quillen, A. C. 2003, *ApJ*, 592, 935  
 Gualandris, A., Portegies Zwart, S., & Sipiør, M. S. 2005, *MNRAS*, 363, 223  
 Gürkan, M. A., Freitag, M., & Rasio, F. A. 2004, *ApJ*, 604, 632  
 Gürkan, M. A. & Rasio, F. A. 2005, *ApJ*, 628, 236  
 Güsten, R. & Philipp, S. D. 2004, in *The Dense Interstellar Medium in Galaxies*, ed. S. Pfalzner, C. Kramer, C. Staubmeier, & A. Heithausen, 253–+  
 Haardt, F., Sesana, A., & Madau, P. 2006, *Memorie della Societa Astronomica Italiana*, 77, 653  
 Hänninen, J. & Flynn, C. 2002, *MNRAS*, 337, 731  
 Hansen, B. M. S. & Milosavljević, M. 2003, *ApJ*, 593, L77  
 Hills, J. G. 1981, *AJ*, 86, 1730  
 —. 1988, *Nature*, 331, 687  
 —. 1991, *AJ*, 102, 704  
 —. 1992, *AJ*, 103, 1955  
 Hirsch, H. A., Heber, U., O’Toole, S. J., & Bresolin, F. 2005, *A&A*, 444, L61  
 Holley-Bockelmann, K., Mihos, J. C., Sigurdsson, S., Hernquist, L., & Norman, C. 2002, *ApJ*, 567, 817  
 Holley-Bockelmann, K. & Sigurdsson, S. 2006, *ArXiv Astrophysics e-prints*  
 Hopman, C. & Alexander, T. 2005, *ApJ*, 629, 362  
 —. 2006a, available at <http://xxx.lanl.gov/abs/astro-ph/0606161>  
 —. 2006b, *ArXiv Astrophysics e-prints*, available at <http://xxx.lanl.gov/abs/astro-ph/0603324>  
 Jenkins, A. & Binney, J. 1990, *MNRAS*, 245, 305  
 Kim, S. S., Figer, D. F., & Morris, M. 2004, *ApJ*, 617, L123  
 Kim, S. S. & Morris, M. 2001, *ApJ*, 554, 1059  
 Knapp, G. R. 1999, in *ASP Conf. Ser. 163: Star Formation in Early Type Galaxies*, ed. P. Carral & J. Cepa, 119–+  
 Kobulnicky, H. A., Fryer, C. L., & Kiminki, D. C. 2006, *ArXiv*, available at <http://xxx.lanl.gov/abs/astro-ph/0605069>  
 Lacey, C. G. 1984, *MNRAS*, 208, 687  
 Lada, C. J. 2006, *ApJ*, 640, L63  
 Lada, C. J. & Lada, E. A. 2003, *ARA&A*, 41, 57  
 Levin, Y. 2005, *ArXiv Astrophysics e-prints*  
 —. 2006, *MNRAS*, submitted, available at <http://xxx.lanl.gov/abs/astro-ph/0603583>  
 Levin, Y. & Beloborodov, A. M. 2003, *ApJ*, 590, L33  
 Levin, Y., Wu, A., & Thommes, E. 2005, *ApJ*, 635, 341  
 Lightman, A. P. & Shapiro, S. L. 1977, *ApJ*, 211, 244  
 Magorrian, J. & Tremaine, S. 1999, *MNRAS*, 309, 447  
 Maillard, J. P., Paumard, T., Stolovy, S. R., & Rigaut, F. 2004, *A&A*, 423, 155  
 Merritt, D. & Poon, M. Y. 2004, *ApJ*, 606, 788  
 Merritt, D. & Quinlan, G. D. 1998, *ApJ*, 498, 625  
 Merritt, D. & Wang, J. 2005, *ApJ*, 621, L101  
 Miller, G. E. & Scalzo, J. M. 1979, *ApJS*, 41, 513  
 Miller, M. C., Freitag, M., Hamilton, D. P., & Lauburg, V. M. 2005, *ApJ*, 631, L117  
 Milosavljević, M. & Loeb, A. 2004, *ApJ*, 604, L45  
 Miralda-Escudé, J. & Kollmeier, J. A. 2005, *ApJ*, 619, 30  
 Miyazaki, A. & Tsuboi, M. 2000, *ApJ*, 536, 357  
 Mouawad, N., Eckart, A., Pfalzner, S., Schödel, R., Moutaka, J., & Spurzem, R. 2005, *Astronomische Nachrichten*, 326, 83  
 Muno, M. P., Bower, G. C., Burgasser, A. J., Baganoff, F. K., Morris, M. R., & Brandt, W. N. 2006, *ApJ*, 638, 183  
 Norman, C. & Silk, J. 1983, *ApJ*, 266, 502  
 Oka, T., Hasegawa, T., Sato, F., Tsuboi, M., Miyazaki, A., & Sugimoto, M. 2001, *ApJ*, 562, 348  
 Paumard, T., Genzel, R., Martins, F., Nayakshin, S., Beloborodov, A. M., Levin, Y., Trippe, S., Eisenhauer, F., Ott, T., Gillessen, S., Abuter, R., Cuadra, J., Alexander, T., & Sternberg, A. 2006, *ApJ*, 643, 1011  
 Polnarev, A. G. & Rees, M. J. 1994, *A&A*, 283, 301  
 Portegies Zwart, S. F., Baumgardt, H., Hut, P., Makino, J., & McMillan, S. L. W. 2004, *Nature*, 428, 724

- Portegies Zwart, S. F., Baumgardt, H., McMillan, S. L. W., Makino, J., Hut, P., & Ebisuzaki, T. 2006, *ApJ*, 641, 319
- Rauch, K. P. & Ingalls, B. 1998, *MNRAS*, 299, 1231
- Rauch, K. P. & Tremaine, S. 1996, *New Astronomy*, 1, 149
- Rees, M. J. 1988, *Nature*, 333, 523
- Rupen, M. P. 1997, in *ASP Conf. Ser. 116: The Nature of Elliptical Galaxies: 2nd Stromlo Symposium*, ed. M. Arnaboldi, G. S. Da Costa, & P. Saha, 322–+
- Schödel, R., Eckart, A., Iserlohe, C., Genzel, R., & Ott, T. 2005, *ApJ*, 625, L111
- Schaller, G., Schaerer, D., Meynet, G., & Maeder, A. 1992, *A&AS*, 96, 269
- Sellwood, J. A. 2002, in *The shapes of galaxies and their dark halos, Proceedings of the Yale Cosmology Workshop "The Shapes of Galaxies and Their Dark Matter Halos"*, New Haven, Connecticut, USA, 28-30 May 2001. Edited by Priyamvada Natarajan. Singapore: World Scientific, 2002, ISBN 9810248482, p.123, ed. P. Natarajan, 123–+
- Serabyn, E. & Morris, M. 1996, *Nature*, 382, 602
- Shields, G. A., Gebhardt, K., Salviander, S., Wills, B. J., Xie, B., Brotherton, M. S., Yuan, J., & Dietrich, M. 2003, *ApJ*, 583, 124
- Spitzer, L. 1987, *Dynamical evolution of globular clusters* (Princeton, NJ, Princeton University Press, 1987, 191 p.)
- Spitzer, L. J. & Schwarzschild, M. 1951, *ApJ*, 114, 385
- . 1953, *ApJ*, 118, 106
- Sternberg, A., Hoffmann, T. L., & Pauldrach, A. W. A. 2003, *ApJ*, 599, 1333
- Stolte, A., Brandner, W., Grebel, E. K., Lenzen, R., & Lagrange, A.-M. 2005, *ApJ*, 628, L113
- Villumsen, J. V. 1983, *ApJ*, 274, 632
- . 1985, *ApJ*, 290, 75
- Völlmer, B., Zylka, R., & Duschl, W. J. 2003, *A&A*, 407, 515
- Young, P. 1980, *ApJ*, 242, 1232
- Young, P. J. 1977, *ApJ*, 215, 36
- Yu, Q. & Tremaine, S. 2003, *ApJ*, 599, 1129
- Zhao, H., Haehnelt, M. G., & Rees, M. J. 2002, *New Astronomy*, 7, 385